Phase transitions in $(NH_4)_2MoO_2F_4$ crystal

Alexander Krylov [a], Natalia Laptash [b], Alexander Vtyurin [a], Svetlana Krylova [a, *]

[a] L.V. Kirensky Institute of Physics SB RAS, Krasnoyarsk, 660036, Russia
[b] Institute of Chemistry FEB RAS, Vladivostok, 690022, Russia

ABSTRACT

The mechanisms of temperature and high pressure phase transitions have been studied by Raman spectroscopy. Room temperature (295 K) experiments under high hydrostatic pressure up to 3.6 GPa for $(NH_4)_2 MoO_2 F_4$ have been carried out. Experimental data indicates a phase transition into a new high-pressure phase for $(NH_4)_2 MoO_2 F_4$ at 1.2 GPa. This phase transition is related to the ordering anion octahedron groups $[MoO_2 F_4]^{2-}$ and is not associated with ammonium group. Raman spectra of small non-oriented crystals ranging from 10 to 350 K have been observed. The experiment shows anion groups $[MoO_2 F_4]^{2-}$ and ammonium in high temperature phase are disordered. The phase transition at $T_1 = 269.8$ K is of the first-order, close to the tricritical point. The first temperature phase transition is related to the ordering anion octahedron groups $[MoO_2 F_4]^{2-}$. Second phase transitions $T_2 = 180$ K are associated with the ordering of ammonium. The data presented within this study demonstrate that 2D correlation analysis combined with traditional Raman spectroscopy are powerful tool to study phase transitions in the crystals.

© 2016 Elsevier B.V. All rights reserved.

1. Introduction

The phase transitions accompanied by the significant entropy changes and the sensitivity of the phase transitions to external pressure allow one to consider oxyfluorides as promising materials to achieve barocaloric effects. This offers new perspectives for using these compounds as active elements of solid-state coolers [1]. Besides barocaloric effect, oxyfluorides possess interesting structural, magnetic and optical effects [2–6]. The polarity of $MeO_2 F_4$ complexes is attractive due to the possibility of obtaining new functional noncentrosymmetric materials with a wide transparency range [7,8].

At room temperature $(NH_4)_2 MoO_2 F_4$ crystals has orthorhombic symmetry (space group Cmcm, Z = 4). $(NH_4)_2 MoO_2 F_4$ has phase transitions at the temperatures $T_1 = 269.8$ K (space group Pnma) and $T_2 = 180$ K [9,10]. Phase transitions in crystals with six-coordinated anions containing F and O are usually associated with lattice instabilities related to rotation of the octahedron groups $[MoO_2 F_4]^{2-}$ and ammonium group ordering process (Fig. 1).

The hydrostatic pressure and uniaxial stress along the b direction induce fairly strong intensive and extensive barocaloric effects [11]. The external pressure is a fairly effective tool for changing the entropy of compounds that contain ordering ions or ionic groups. The method of Raman spectroscopy can be an additional powerful tool for studying phase transitions. This method allows one to estimate the role of molecular groups in the phase transition mechanism and character of phase transitions. In particular, temperature and baric phase transitions in other oxyfluorides [12,13] were studied by Raman spectroscopy.

The present paper describes the temperature and pressure dependent structural changes in $(NH_4)_2 MoO_2 F_4$ by using Raman spectroscopy to clarify the phase transition mechanisms.

2. Experimental

The single crystals of $(NH_4)_2 MoO_2 F_4$ were synthesized through $(NH_4)_3 MoO_3 F_3$ obtained from a mixture of ammonium molybdate aqueous solution with a concentrated solution of $NH_4 F$. The resulting excess white precipitate of $(NH_4)_3 MoO_3 F_3$, which can contain an impurity of $(NH_4)_2 MoO_3 F_2$, was dissolved in an aqueous solution of HF. The transparent solution was then slowly evaporated in air, and well shaped single crystals of $(NH_4)_2 MoO_2 F_4$ in the form of prisms or thick plates were obtained [2].

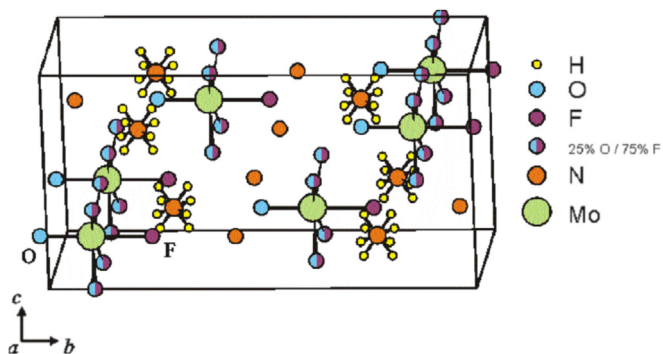Raman spectra were acquired using a Horiba Jobin Yvon T64000 spectrometer in backscattering geometry. The spectra were excited

Fig. 1. Unit cell structure of $(NH_4)_2 MoOF_4$ in the orthorhombic phase.

using an Ar + laser (wavelength of 514 nm) with the power of 20 mW, corresponding to a laser power density of 60 W/cm^2. Temperature measurements were taken by a closed-cycle helium cryostat ARS CS204-X1.SS. The temperature was controlled using a calibrated silicon diode LakeShore DT-6SD1.4L. The temperature stabilization accuracy was better than 0.2 K. The sample was placed in the indium gasket, with one side being opened and then mounted on the cold finger. During the experiments, the cryostat was pumped to a pressure of 1.0×10^{-6} mBar.

The experiments were carried out under the conditions of high hydrostatic pressure at room temperature (295 K), using a diamond anvil cell with the sample chamber diameter of 0.25 mm and height of 0.2 mm. The pressure to the accuracy of 0.05 GPa was determined by the shift of the luminescence line $^2F_g \rightarrow {}^4A_{2g}$ of the Cr^{3+} ion of a ruby [15,16] microcrystal located near sample.

Pressure decompression brings crystal to the initial state. All the changes observed are reversible and can be reproduced with different samples taken from the same crystallization, within the experimental error (about 0.05 GPa).

3. Disscussion

The full spectrum of the crystal $(NH_4)_2 MoO_2 F_4$ at 295 K and 10 K is presented in Fig. 2. A high degree of the ionic group disorder does not allow a full theoretical and group analysis. We divided the spectrum into the next parts: up to 200 cm^{-1} lattice vibrations; in the range from 200 to 700, stretching Mo−F vibrations and bending O(F)−Mo−O(F) vibrations of the $[MoO_2 F_4]^{2-}$ ions; in the range from 750 to 1100 cm^{-1}, stretching Mo−O vibrations of the $[MoO_2$
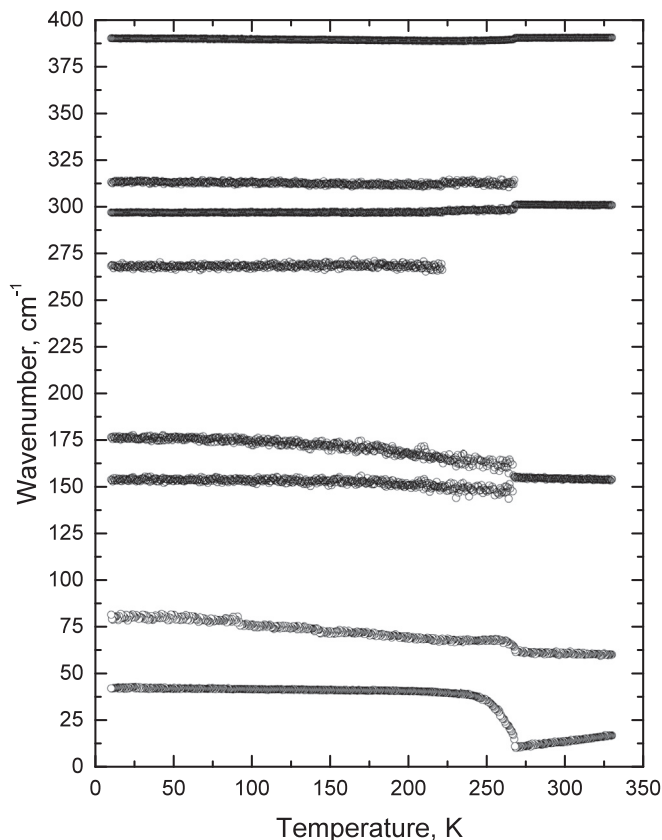

Fig. 3. Dependencies of the line positions on temperature in the range from 0 to 400 cm^{-1}

$F_4]^{2-}$ ions; in the range from 1300 to 1800 cm^{-1}, ammonium bending vibrations; in the range from 2500 cm^{-1} to 3500 cm^{-1}, ammonium stretching vibrations are observed. The dependency of the line positions on temperature in the range from 0 to 400 cm^{-1} is presented in Fig. 3. New modes near 150 cm^{-1} and 300 cm^{-1} appear after the transition lower $T_1 = 270$ K. In the range from 250 to 400 cm^{-1}, one can observe the stretching and bending vibrations of Mo−F as well as the bending vibrations of O−Mo−O. Up to the temperature $T_1 = 270$ K, the positions of all the lines behave monotonically (Fig. 3). As additional information we included the
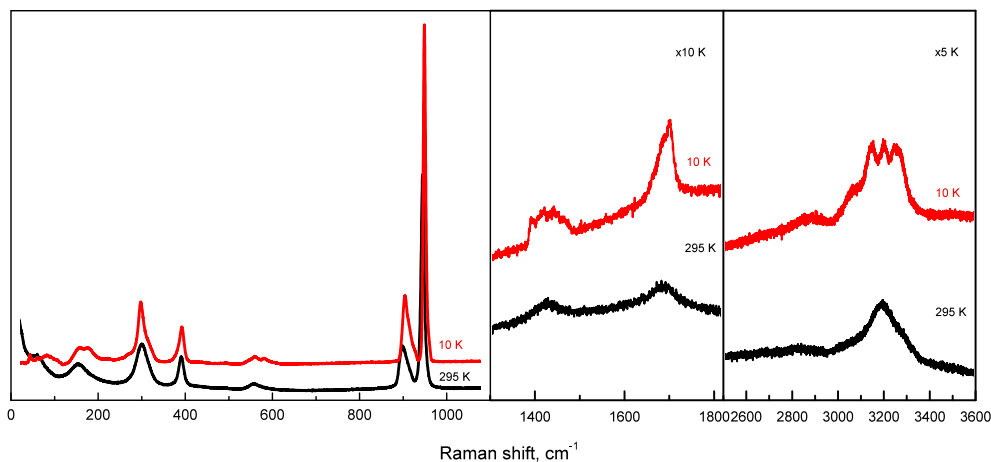

Fig. 2. Raman spectra of crystal $(NH_4)_2 MoO_2 F_4$ at 295 K and 10 K.

390 cm^{-1} mode and wide of line behavior with temperature increasing in Fig. S1 (Supporting information). In the range from 525 to 600 cm^{-1}, one can observe stretching Mo−F vibrations and bending O(F)−Mo−O(F) vibrations (Fig. 4) New mode near 575 cm^{-1} appear after the transition $T_1 = 270$ K. One can observe stretching Mo−O vibrations of the $[MoO_2 F_4]^{2-}$ ions in the region from 875 to 975 cm^{-1} (Fig. 4). The line position of the 890 cm^{-1} mode shifted. However, we did not find anomalies in the spectra are observed associated with the second phase transition $T_2 = 180$ K in the range of the lattice vibrations, stretching vibrations Mo−F, and bending ones O−Mo−O. The significant wavenumber shift of the most low wavenumber indicates that the first transition is of the first order.

The anomalous behavior of the lowest wavenumber mode (24 cm^{-1} at 295 K) deserves particular consideration. The low wavenumber modes is connected with vibration of heavy Mo ion and lattice vibration. Fig. 5 shows the temperature dependence of the position of the low wavenumber mode, the behavior of the width of the line width with temperature and square of the wavenumber $\omega^2 \equiv \omega_0^2 - \gamma^2$. At 270 K, the line position increases by a jump from 24 to 36 cm^{-1} (Fig. 5). The line width increases from 4 to 24 cm^{-1} and decreases abruptly to 15 cm^{-1} (Fig. 5). Such an abrupt change of the wavenumbers and linewidths indicates that there is a first-order phase transition. The similar behavior of the line width is observed in the oxyflouride $Rb_2 KMoO_3 F_3$ and $(NH_4)_2 WO_2 F_4$ in the first-order transition [13,14].

The normal modes of vibration of a free NH_4^+ ion of Td symmetry have wavenumbers of 1397 (F_2), 1680 (E), 3040 (A_1), and 3145 (F_2) cm^{-1} modes [17]. The modes of the ammonium vibrations are of very low intensive (Fig. 2). We expected the splitting of the
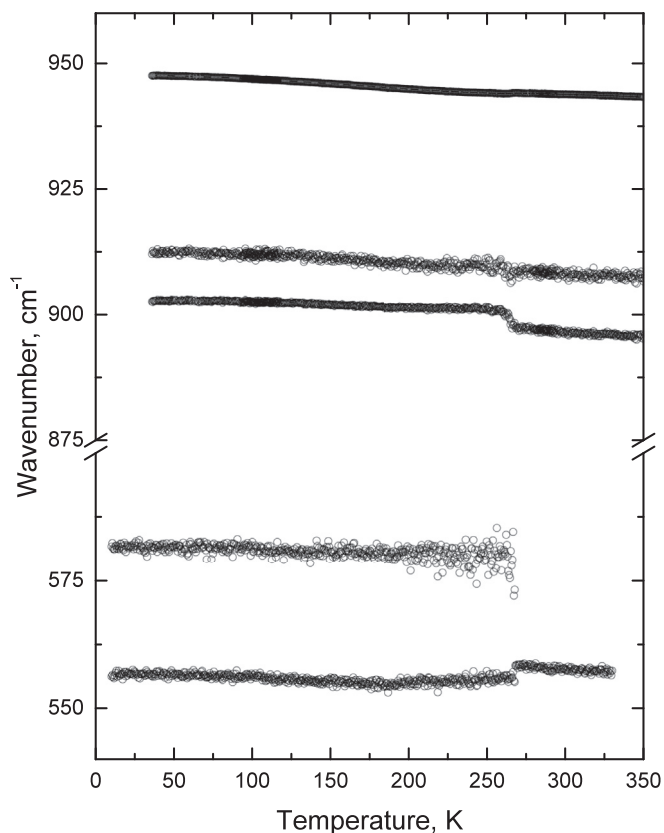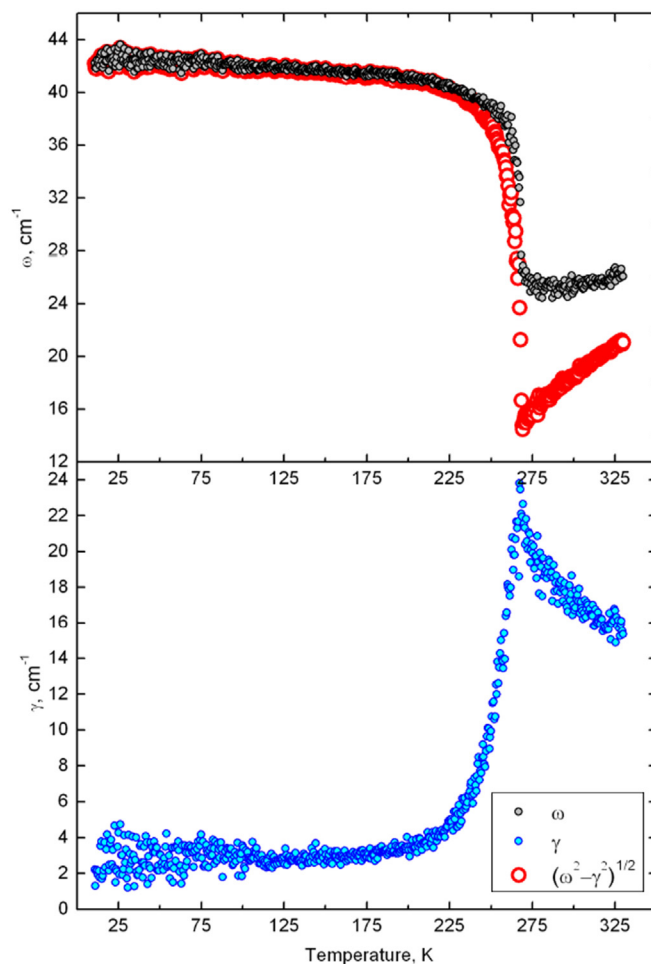

Fig. 5. Temperature dependence of the position of the low wavenumber mode, temperature dependence of full width at half maximum, and temperature dependence of the effective wavenumber.

degenerated modes at 3150 cm^{-1}, 1410 (F_2) and 1700 (E) in the low-symmetry phases. The changes in the spectra of the ammonium ion stretching vibrations with temperature are given in Fig. 6. The spectral profile becomes complex with decreasing temperature below T_2. The main changes in the range of the ammonium vibrations occur at temperatures below the second-phase transition. The phenomena observed can be accounted for by the fact that cooling the crystal below the phase transition temperature results in the ordering of the ammonium groups.

Pressure decompression brings crystal to the initial state. All the changes observed are reversible and can be reproduced with different samples taken from the same crystallization, within the experimental error (about 0.05 GPa). The positions and width of lines are changed insignificantly in the ammonium parts of spectra with pressure increasing. The low wavenumber part of the spectrum under pressure increasing is presented in Fig. 7. A new modes arrive under the pressure 1.2 GPa (150 and 270 cm^{-1}). One can see significant changes in the part of the spectrum associated with Mo−O vibrations in Fig. 8. The slope of the pressure dependencies of the line positions at 900 and 913 cm^{-1} changes near 1.2 GPa. The low wavenumber mode dependence on pressure is presented in Fig. 9. The low wavenumber mode (15 cm^{-1}) change of the slope at 1.2 GPa connected with phase transition. The transformation of the low vavenumber part from 10 to 650 cm^{-1} is included in the supporting materials (Fig. S2). The changes of spectrum with pressure
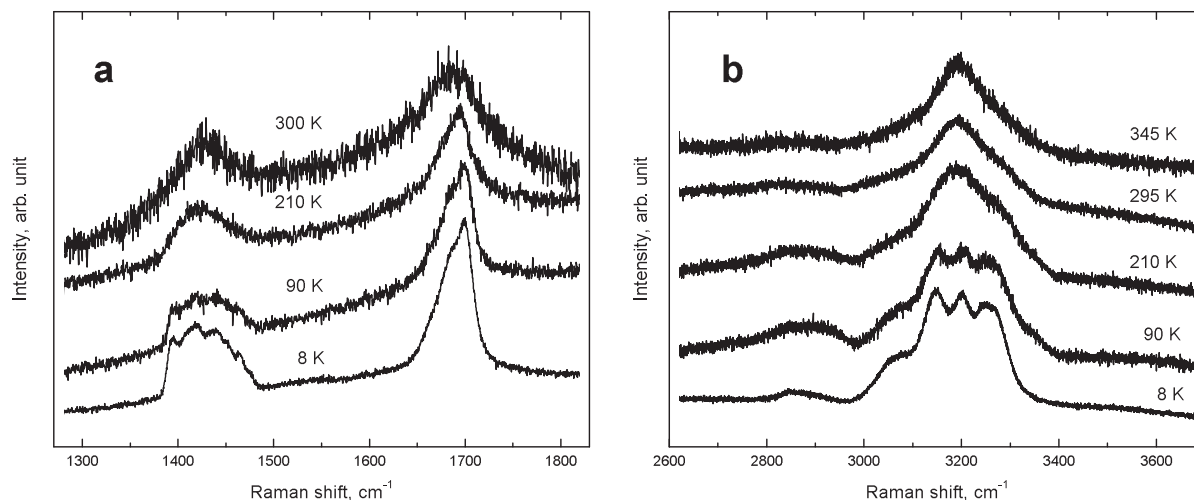

Fig. 4. Dependencies of the line positions on temperature in the range from 525 to 975 cm^{-1}

Fig. 6. Raman spectra transformation with changing temperature in the range a) from 1300 to 1800 cm^{-1} b) from 2600 to 3600 cm^{-1}
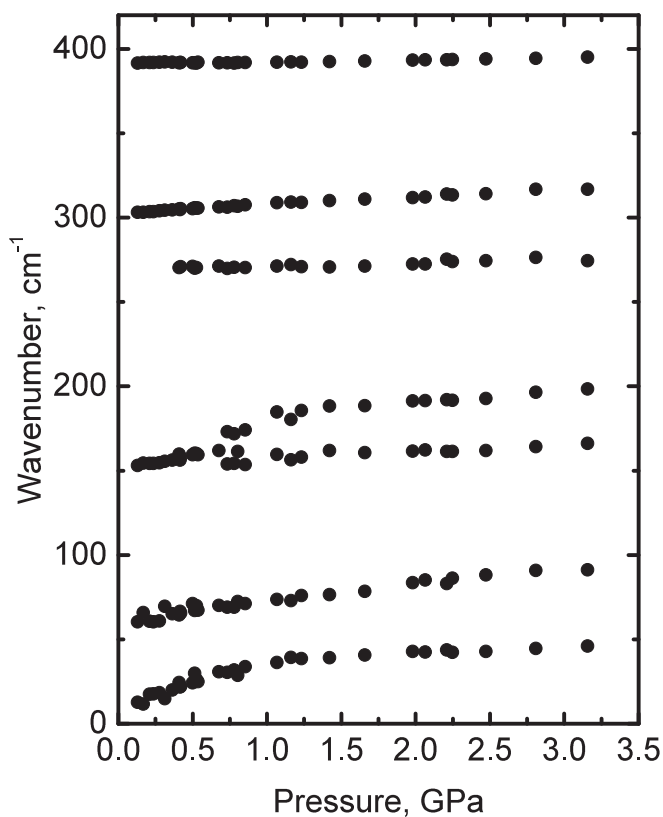

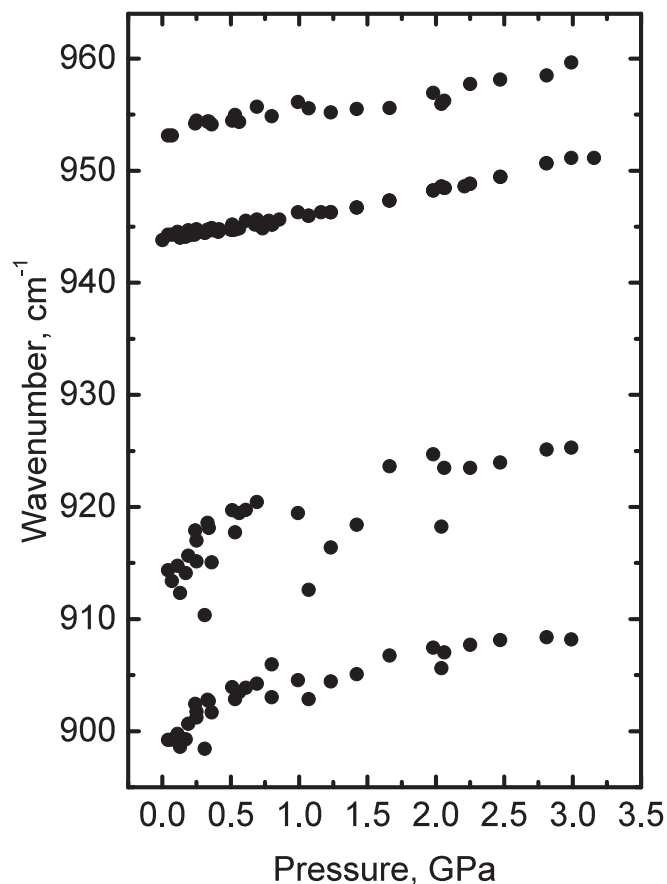**Fig. 7.** Pressure dependence of line positions in the range from 0 to 400 cm^{-1}

Fig. 8. Pressure dependence of line positions in the range from 850 to 970 cm^{-1}

increasing in the region from 875 to 975 cm^{-1} is included in the supporting information (Fig. S3). The transformation of ammonium vibration under pressure increasing is presented in Fig. S4 and Fig. S5 (supporting information).

Data that is evenly spaced along the perturbation variable is generally required to perform 2D correlation analysis. As all bands in Raman spectra are of the same positive sign, interpretation of the 2DCos Raman synchronous and asynchronous plots to determine sequence order of band changes is, relatively, straightforward following Noda's rules [18]. Using Noda's rules of interpretation, positive synchronous cross peaks indicate that both spectral bands change intensity in the same direction, either both increasing or decreasing, whereas negative cross peaks (which are shaded gray in these figures) indicate that both bands change in opposite direction, one band increasing in intensity and the other decreasing. Relating these contours to their structural origins is a relatively simple process for intensity variations in the positive intensity range of spectra.

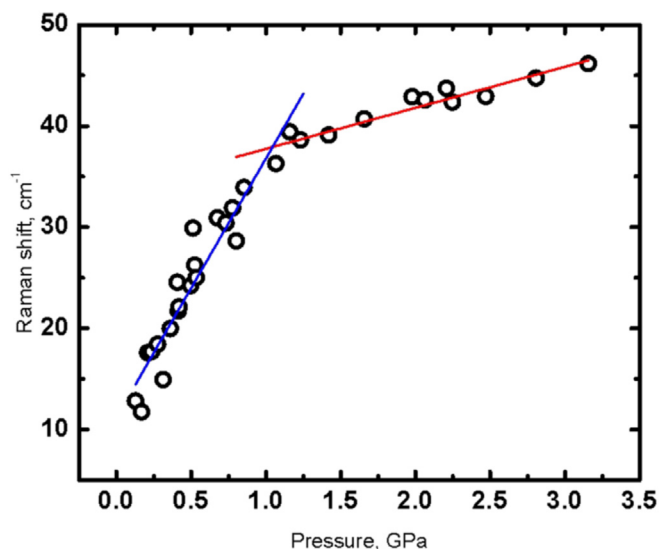The 2D correlation is a data analysis technique useful for the

Fig. 9. Pressure dependence of peak positions of the lowest wavenumber mode.

examination of systematic variations of almost any reasonable analytical signals observed with a variety of spectroscopic probes, e.g., IR, Raman, X-ray, and NMR, as well as those from chromatography or microscopy studies. In 2D correlation, the variation of an analytical signal is induced by imposing an external perturbation selected from a large list of possibilities, e.g., mechanical, electrical, thermal, chemical, biological, and many more, to the sample system of interest [19–21].

To retrace the changes connected with phase transitions we divided temperature region on three parts and calculated 2D Raman correlation spectra between 10 and 170 K for phase G_2, between 180 and 260 K for phase G_1 and between 270 and 340 K for phase G_0 (in steps of 10 K) in the wavenumber region between 10 and 1000 cm^{-1}. As expected from temperature-dependent Raman spectra, there are four Raman peaks at 948, 861, 378, 265 cm^{-1} in G_0 phase, which showed the largest temperature-dependent intensity variations (Fig. 10). One can see the four auto peaks and off-−diagonal correlations. The crosspeaks 861/948, 378/948, 265/948 cm^{-1} are positive, the intensities at corresponding wave-numbers are increasing (or decreasing) together with temperature changes. The wavenumber region between 860 cm^{-1} and 980 cm^{-1}
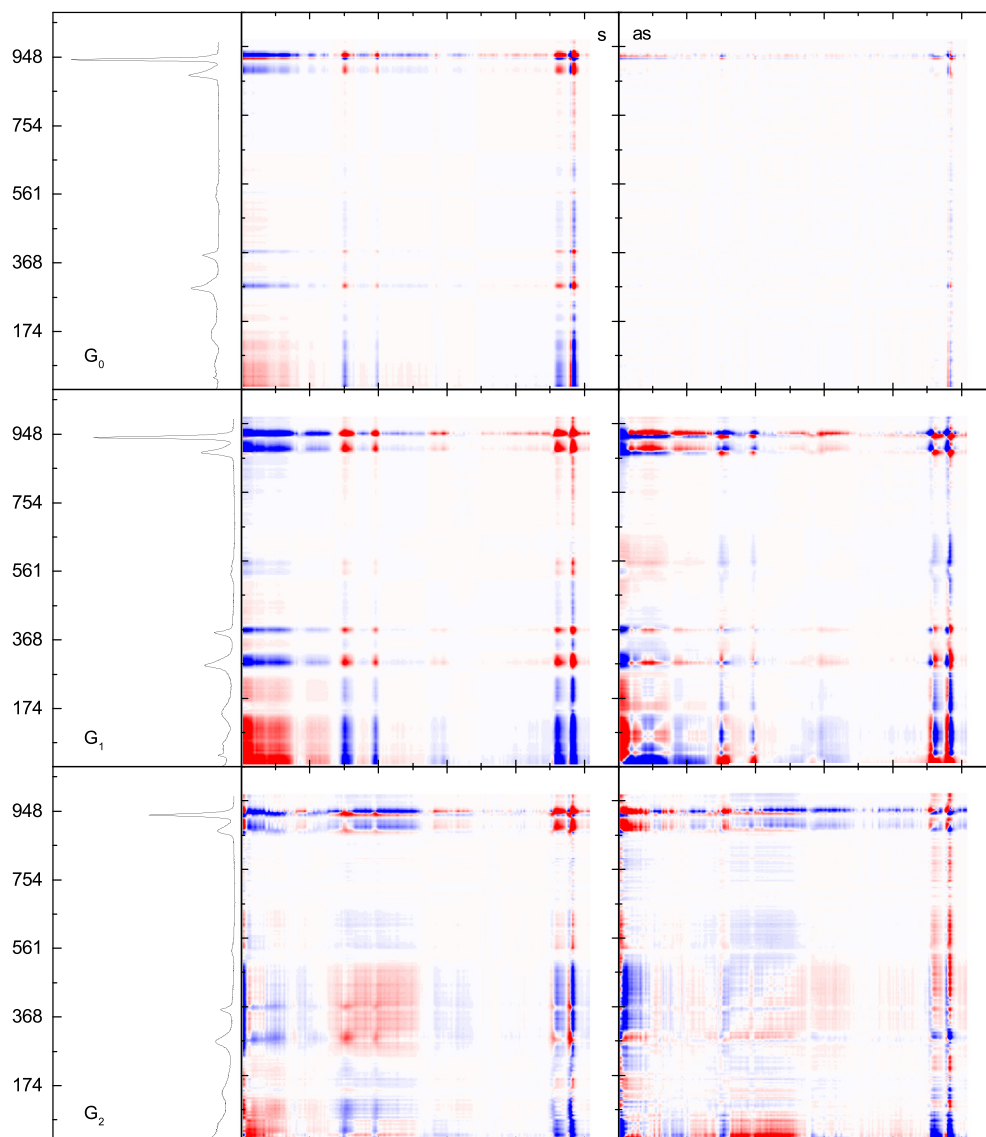

Fig. 10. Synchronous (left) and asynchronous (right) 2D Raman correlation spectra between 10 and 170 K for phase G_2, between 180 and 260 K for phase G_1 and between 270 and 340 K for phase G_0 (in steps of 10 K) in the wavenumber region between 10 and 1000 cm^{-1}. Red color indicates positive peaks, while blue shows negative ones.

consist of the bands connected with stretching Mo—O vibrations of the $[MoO_2 F_4]^{2-}$ ions. The observed temperature-dependent Raman spectra were 2D correlated in this region. (see Fig. 10). The 2D correlation synchronous and asynchronous spectra contain clearly resolved peaks. Four-leaf clover pattern for two autopeaks and two negative crosspeaks in the synchronous spectrum and the "butterfly" in the asynchronous spectra is classic pattern of the line shift. This interpretation of the band at 948 cm^{-1} is only possible using the 2D correlation analysis. One can see significant changes after first phase transition as in synchronous spectra as in the asynchronous spectra in G_1 phase. In the low wavenumber part one can see two autopeaks at 42 and 75 cm^{-1} in the synchronous spectrum. The crosspeaks 861/42 (75), 948/42 (75), 378/42 (75), 265/42 (75) cm^{-1} are negative, the intensities at corresponding wavenumbers (42, 75 cm^{-1}) (lattice vibrations) are increasing, while the other (ion groups vibrations) is decreasing with temperature decreasing. The changes of the correlation spectra are rather interesting in G_2 phase. One can see the autopeak at 24 cm^{-1} instead at 42 cm^{-1}. The noticeable shift points to the first order phase transition changes. The autopeak at 75 cm^{-1} almost disappointed. The intensity of this band practically didn't change in this temperature region. The 2D correlation analysis helped us in finding the changes between G_1 and G_2 phases, while traditional Raman spectroscopy investigation didn't allow to find them. The additional information about ion groups intensity behavior with temperature changes was received from this analysis.

4. Conclusion

In summary, a new high-pressure phase transition at 1.2 GPa have been found and mechanisms of temperature phase transitions at T1 = 269.8 K, T2 = 180 K have been studied using Raman spectroscopy technique. The anion groups and ammonium ions in the high-temperature phase are disordered orientationally, which is evidenced by wide internal lines and weak temperature dependence of these widths far from the transition point T_1. The phase transition T_1 is of the first-order, close to the tricritical point. The temperature phase transition T_1 is due to the ordering of the anion groups of $[MoO_2 F_4]^{2-}$ and ammonium groups, while the phase transition T_2 is due to the ammonium ordering. The high-pressure phase transition is associated with the ordering of the $[MoO_2 F_4]^{2-}$ ions.

In this study — the first Raman spectroscopic 2D correlation analysis of oxyfluorides is presented. We show that this approach is promising for analyzing and understanding phase transition in disordered crystals more precisely compared to using normal Raman spectroscopy by its own.

Appendix A. Supplementary data

Supplementary data related to this article can be found at http://dx.doi.org/10.1016/j.molstruc.2016.03.009.

References

[1] N.A.J. Oliveira, Appl. Phys. 109 (2011) 053515.
[2] M. Leblanc, V. Maisonneuve, A. Tressaud, Chem. Rev. 115 (2) (2015) 1191–1254.
[3] V.V. Atuchin, L.I. Isaenko, V.G. Kesler, Z.S. Lin, M.S. Molokeev, A.P. Yelisseyev, S.A.J. Zhurkov, Solid State Chem. 187 (2012) 159–164.
[4] V.V. Atuchin, M.S. Molokeev, G.Yu Yurkin, T.A. Gavrilova, V.G. Kesler, N.M. Laptash, I.N. IFlerov, G.S. Patrin, J. Phys. Chem. C 116 (2012) 10162–10170.
[5] T. Mori, K. Kajihara, K. Kanamura, Y. oda, H. Hiramatsu, H. Hosono, J. Am. Chem. Soc. 135 (35) (2013) 13080–13088.
[6] V.V. Atuchin, T.A. Gavrilova, L.I. Isaenko, V.G. Kesler, M.S. Molokeev, S.A. Zhurkov, Ceram. Int. 38 (2012) 2455–2459.
[7] S.V. Mel'nikova, N.M. Laptash, Phys. Solid State 57 (2015) 1201–1205.
[8] E.V. Bogdanov, E.I. Pogoreltsev, S.V. Mel'nikova, M.V. Gorev, I.N. Flerov, M.S. Molokeev, A.V. Kartashev, A.G. Kocharova, N.M. Laptash, Phys. Solid State 55 (2013) 409–418.
[9] V.D. Fokina, E.V. Bogdanov, E.I. Pogorelcev, V.S. Bondarev, I.N. Flerov, N.M. Laptash, Phys. Solid State 52 (2010) 158.
[10] A.A. Udovenko, A.D. Vasiliev, N.M. Laptash, Acta Cryst. B 66 (2010) 34–39.
[11] M.V. Gorev, E.V. Bogdanov, I.N. Flerov, A.G. Kocharova, N.M. Laptash, Phys. Solid State 52 (2010) 167–175.
[12] A.S. Krylov, S.V. Goryainov, A.N. Vtyurin, S.N. Krylova, S.N. Sofronova, N.M. Laptash, T.B. Emelina, V.N. Voronov, S.V.J. Babushkin, Raman Spectrosc. 43 (2012) 577–582.
[13] A.S. Krylov, S.V. Goryainov, N.M. Laptash, A.N. Vtyurin, S.V. Melnikova, S.N. Krylova, Cryst. Growth Des. 14 (2014) 374–380.
[14] A.S. Krylov, E.M. Kolesnikova, L.I. Isaenko, S.N. Krylova, A.N. Vtyurin, Cryst. Growth Des. 14 (2014) 923–927.
[15] R.G. Munro, G.J. Piermarini, S. Block, W.B.J. Holzapfel, Appl. Phys. 57 (1985) 165.
[16] W.L. Vos, J.A.J. Schouten, Appl. Phys. 69 (1991) 6744.
[17] K. Nakamoto, Infrared and Raman Spectra of Inorganic and Coordination Compound, John Wiley and Sons, New York, 1986.
[18] I. Noda, Appl. Spectrosc. 47 (1993) 1329–1336.
[19] I. Noda, J. Mol. Struct. 1069 (2014) 3.
[20] I. Noda, J. Mol. Struct. 1069 (2014) 23.
[21] J. Popp, R. Geitner, J. Kötteritzsch, M. Siegmann, T. Bocklitz, M. Hager, U.S. Schubert, S. Graefe, B. Dietzek, M. Schmitt, Phys. Chem. Chem. Phys. 17 (2015) 22587–22595.